PPPL-3163 - Preprint Date: February 1996, UC-420, 426

Observation of Non-Classical Radial Current Diffusion in a Fully Bootstrap Current Driven Tokamak

Y. S. Hwang, C B. Forest[#] , and M. Ono
Princeton University, P.O. Box 451, Princeton, NJ 08543

ABSTRACT

Reconstruction and modeling of the plasma current profiles in a fully pressure-driven tokamak have been performed in the Current Drive Experiment-Upgrade(CDX-U). The reconstructed experimental current profile has a significant deviation from that of the calculated neoclassical currents. Satisfactory agreement between the measured and calculated model profiles was obtained by including a helicity conserving current diffusion term in the modeling which created the required self-generated “seed” current.

For future long-pulse and/or steady-state tokamaks, internally generated bootstrap current is expected to play a major role since it could reduce the requirements for non-inductive current drive. Theoretical estimates show that a large fraction of plasma current is expected to flow as bootstrap current in high beta-poloidal (b_{pol}) reactor-grade plasmas.[1] Recent experimental observations in high-b_{pol} tokamak plasmas heated by Neutral Beam Injection (NBI),[2,3] Electron Cyclotron Heating (ECH),[4] and Ion Cyclotron Range of Frequency (ICRF)[5] support this prediction. It is generally believed that the bootstrap current requires a "seed" current near the plasma magnetic axis since no neoclassical current is expected to be generated there except in limited conditions.[6] However, the possibility of sustaining tokamak plasmas solely by bootstrap current has been suggested previously.[7,8] Several non-classical mechanisms of transporting the bootstrap current to the magnetic axis have been proposed, thereby permitting bootstrap current to be self-sustained. A fully self-sustaining tokamak, if possible, is indeed very attractive as a simple economic reactor option. It has been reported that the flux surface closure was achieved in the CDX-U experiment entirely by pressure-driven currents ($I_p \leq$ 1kA).[9] With discharge optimization, up to 2.4 kA of pressure driven current has been obtained from zero current when non-phased 8 kW of ECH power was used to create and maintain a hot, low-collisionality electron plasma for the duration of the heating pulse which is much longer than the magnetic resistive decay time. An important question we attempt to answer in this letter is how such a plasma can be generated and sustained self-consistently, and how well the existing neoclassical or other theoretical models explain the experimental observation. For this investigation, we have developed and applied a two-dimensional profile reconstruction technique from detailed magnetic and kinetic diagnostic systems, and compared with the neoclassical model calculations. A crucial discrepancy between experimental observation and neoclassical model lies in the current profiles, where the former shows smooth and non-hollow and the latter shows hollow characteristics. In this letter, we report that satisfactory agreement between the measured and calculated profiles is obtained when the helicity conserving current diffusion term of Boozer[10] is included in the modeling. This result supports the existence of a non-classical helicity conserving current transport mechanism which generates "seed" current near the plasma axis to sustain a fully pressure-driven tokamak discharge.[7,8]

The investigation was performed in the Princeton CDX-U device (R = 34 cm, a = 23 cm).[9] To model the neoclassical currents, two dimensional magnetic field structure and pressure profiles are required. The current density distributions are reconstructed from internal and external magnetic measurements from the magnetic diagnostic array as shown in the right of Fig.1(a).[11] Three-dimensional magnetic pick-up coils, located at 13 different poloidal positions, measure the vector magnetic field. Three flux loops are wound around the central toroidal field column (center stack) to provide poloidal magnetic flux measurements at the inside boundary. Nine one-dimensional pick-up coils are located near the center stack to measure the vertical magnetic field. A two-dimensionally scannable magnetic probe system[12] maps poloidal magnetic fields radially from R=36 cm to R=60 cm and vertically from Z=-13 cm to Z=16 cm. Since the internal magnetic probe has limited scanning ranges and perturbs the plasma significantly if inserted into the core of the high current plasmas, the full internal magnetic structure could not be measured by the internal magnetic probe alone. However, the external magnetic measurements described above together with the internal probe measurements can reconstruct the current density distributions by taking advantage of the low-aspect-ratio nature of the plasma, utilizing least squares error technique and finite element method.[11,13,14] Reconstructed current density and magnetic flux contours are shown in Fig. 1(b). Formation of a low-aspect-ratio tokamak configuration can indeed be seen. Electron density profiles are measured two-dimensionally by a 140 GHz interferometer system.[15] This microwave interferometer scans horizontally from 26 cm to 55 cm and vertically from -22 cm to +22 cm, which is limited by the size of rectangular ports on the vacuum vessel. An additional channel is installed inside the vacuum vessel at R=17 cm. Imposing the known magnetic structure as a grid, a tomographic inversion of electron density was performed by using least squares

error technique.[14] The reconstructed density profile agreed well with the local Langmuir probe measurements as shown in Fig.2(a). The radial profile of electron temperature shown in Fig. 2(b) was obtained at mid-plane by using a small cylindrical Langmuir probe made of 0.4 mm tungsten wire. These density and temperature profiles with the reconstructed magnetic structure are used to model neoclassical currents.

We first describe the physics of neoclassical current generation in CDX-U. A toroidal mirror configuration shown in Fig. 1(a) has been utilized to provide initial confinement for a hot, ECH-produced, trapped electron population.[9] For the open field line configuration, precessional current comprises most of the toroidal current. Given the pressure profile and the poloidal field strength, the precessional current density can be estimated as $J_{prec} \approx P_e/RB_{pol}$ where P_e, R and B_{pol} are electron pressure, major radius and poloidal field, respectively.[16] It is important to note the role of the Pfirsch-Schluter (P-S) current which is generated by the pressure gradients. This current consists of a co-directed current in the outer region and a counter-directed current in the inner region, producing a negative vertical field in the central region. Although the P-S current itself does not carry a significant net toroidal current, it reduces the vertical field substantially in the central high pressure region, which can then enhance precession current as much as a factor of two. With inclusion of both precessional and Pfirsch-Schluter currents, the estimated neoclassical current level agrees satisfactorily with the measured total plasma current in this low-current, open-field-line configuration.

After the closed flux surface formation, previously trapped electrons start to be detrapped and become passing particles since mirror ratio generally decreases inside the flux tube. With increasing numbers of passing particles, the bootstrap current becomes a major contributor to the plasma current while precession current contribution tends to decrease. Indeed, after the closing of the flux surface ($I_p \approx 600$ A), the current can spontaneously increase further to $I_p \approx 2.2$ kA due to bootstrap current. The bootstrap current J_{bs} at an arbitrary aspect ratio is given in Ref. 17. Here ions are considered to be cold. In addition, when there is an in-out asymmetry of electron density in the same flux surface, electrostatic trapping can take place and enhance neoclassical transport.[18] After taking various effects into account, we still find the measured total plasma current in this closed-field-line configuration to be larger by $\approx$ 20% than the calculated total neoclassical currents. The collisional effect, though not included in our model due to low collisionality, tends to reduce the bootstrap current and, thus, cannot explain this discrepancy. However, this 20% systematic deviation is still within the experimental uncertainly in estimating the effective T_e in the ECH heated discharges using a Langmuir probe.

The most significant discrepancy between measurements and neoclassical model, however, is in the qualitative nature of the current profiles. The expected current density profiles calculated from neoclassical theory show a hollow characteristic whereas the reconstructed current density profiles are non-hollow as shown in Fig.2(c). The mid-plane vertical magnetic field measured by the internal probe also supports this deviation. To resolve this discrepancy, non-classical current transport is considered. An anomalous viscosity term is introduced into Ohm's law with the helicity conserving form[10] as following:

$$\vec{E} + \vec{u} \times \vec{B} = \eta(\vec{j} - \vec{j}_{nc}) - \frac{\vec{B}}{B^2} \nabla \cdot (\lambda \nabla j_{\ddot{o}} / B)$$

with h the classical Spitzer resistivity, $\vec{j}_{nc}$ the neoclassical current density and $\vec{j} = (j_{\ddot{o}} / B)\,\vec{B}$ the current density. The hollow current profile, for example, is generally believed to be unstable against the double tearing mode which can induce the non-classical current diffusion.[19] This non-classical diffusion term can redistribute current to the magnetic axis, so that non-hollow current density profiles can be obtained. Here, l represents a current viscosity which determines the current density profile for a given

pressure profile. With this non-classical current penetration, self-consistent modeling is attempted. Parallel force balance from Ohm's law with Faraday's law and Ampere's law gives a current transport equation,

$$\frac{\partial j_{\ddot{o}}}{\partial t} = \frac{\eta}{\mu_o}\nabla^2 (j_{\ddot{o}} - j_{nc}) - \frac{1}{\mu_o}\nabla^2 \left[\frac{1}{B_T}\nabla \cdot \left(\lambda \nabla \frac{j_{\ddot{o}}}{B_T} \right) \right]$$

assuming $B \approx B_T$. Using the calculated neoclassical current j_{nc} as an initial value for each time step, the current transport is estimated with the time step of $10^{-3}\ \tau_s$. Here, a plasma skin time is $\tau_s = \mu_o a^2 / \eta$. The neoclassical current is recalculated for the new magnetic structure obtained from the updated current density $j_{\ddot{o}}$, so self-consistent current density profiles are obtained for different l values as shown in Fig.3 (a). The vertical fields at the mid-plane from these current density profiles are compared with the fields measured by the internal magnetic probe. Fig.3 (b) shows the comparison for different l values. With a small value of l, non-classical current transport is not sufficient to balance the bootstrap effect which tends to push the poloidal magnetic field out of the regions of high plasma pressure as shown in Fig.3 (b) and makes a current density profile become more hollow as time goes on. In this case, plasma current should not be maintained longer than the resistive time scale, which is inconsistent with our experimental observations. With the sufficient non-classical current transport of a larger viscosity, non-hollow profiles are maintained. However, too large viscosity tends to move current density toward high field side, which is inconsistent with magnetic measurements as shown in Fig.3 (b). The non-hollow profile with anomalous viscosity of about 20 % of $[R_o^2 B_o^2 \eta]$ shows a good agreement with the experimental measurements. Other possible mechanisms for generating the central "seed" currents are externally provided electric fields and finite particle banana effects.[8] The only possible electric field is from the vacuum vessel eddy currents. However, its magnitude is too small to generate sufficient central current density. Also, the width of electron bananas is relatively large (about one cm), but much smaller than plasma minor radius. This excludes the possibility of finite banana effects.

In conclusion, a fully bootstrap current driven tokamak plasma was examined using a self-consistent model utilizing reconstructed 2-D pressure and magnetic flux profiles. By introducing a helicity conserving non-classical current transport model, the observed self-maintenance of neoclassical bootstrap currents was explained. This finding supports earlier theoretical predictions of a tokamak discharge maintained entirely by internally generated currents.[7,8] The physics of non-classical current transport may also play an important role during current profile control in advanced tokamaks.[20]

The authors would like to acknowledge the CDX-U group. Also, Drs. S.C. Jardin and C.S. Chang have provided helpful suggestions. This work was supported by the U.S. Department of Energy under Contract No. DE-AC02-76-CHO-3073.

REFERENCES

[1] R. J. Bickerton, J. W. Connor, and J. B. Taylor, Nature(London) Physical Society **229**, 110 (1971).
[2] M. C. Zarnstorff et al., Phys. Rev. Lett. **60** , 1306 (1988).
[3] M. Kikuchi, Nuclear Fusion **30**, 265 (1990).
[4] V. Alikaev et al., AIP Conference Proceedings 244 - Radio Frequency Power in Plasmas, Charleston, SC}, page 11, 1991.
[5] C. D. Challis, T. C. Hender, J. O'Rourke, et al., High bootstrap current ICRH plasmas in JET, Technical Report JET-P(92)76, Joint European Torus, 1992.
[6] C. S. Chang, in Proceedings of the 14th IAEA Conference, Wurtzburg, Germany, (Sept. 1992), (IAEA, Vienna, Austria, 1993) Vol. I, 759.
[7] R. H. Weening and A. H. Boozer, Phys. Fluids B **4**, 159 (1991).
[8] Ya. I. Kolesnichenko, D. Anderson, M. Lisak, and H. Wilhelmsson, Phys. Rev. Lett. **53**, 1825 (1984).
[9] C. B. Forest, Y. S. Hwang, M. Ono and D. S. Darrow, Phys. Rev. Lett. **68**, 3559 (1992).
[10] A. H. Boozer, J. Plasma Phys. **35**, 133 (1986).
[11] Y. S. Hwang, C. B. Forest, D. S. Darrow, G. Greene, and M.Ono, Rev. Sci. Instrum. **63**, 4747 (1992).
[12] G. J. Greene and M. Ono, Bull. Am. Phys. Soc. **34**, 1993 (1989).
[13] F. Hofmann and G. Tonetti, Nuclear Fusion **28**, 519 (1988).
[14] Y.S. Hwang, Ph.D. Thesis, Princeton University (1993).
[15] C. B. Forest, G. J. Greene, and M. Ono, Rev. Sci. Instrm. **61**, 2888 (1990).
[16] K. Miyamoto, Plasma Physics for Nuclear Fusion, pages 65-70, MIT Press, Cambridge, Mass., 1976.
[17] S. P. Hirshman, Phys. Fluids **31**, 116 (1988).
[18] C. S. Chang, Phys. Fluids **26**, 2140 (1983).
[19] T. H. Stix, Nucl. Fusion **18**, 353 (1978).
[20] R. J. Goldston et al., in Proceedings of the 20th European Conference on Controlled Fusion and Plasma Physics, Lisbon, 1993 (European Physical Society, Lisbon, Portugal, 1993), p. I-319.

FIGURE CAPTIONS

Fig. 1. CDX-U cross-sectional views. (a) A schematic of CDX-U experimental set up. The left side shows isolated limiters around the poloidal direction and ECH set-up, and right side is magnetic diagnostics including two-dimensional scanning probe. (b) Magnetic flux and current density contours reconstructed from the magnetic diagnostic data.

Fig. 2. Measured and reconstructed mid-plane profiles. (a) Density profiles reconstructed from the two-dimensional interferometer system with local Langmuir probe data shown for comparison. (b) Electron temperature profile reconstructed from the Langmuir probe data. (c) Comparison of the reconstructed and calculated neoclassical current density profiles.

Fig. 3. Non-classical current diffusion. (a) Current density profiles at the mid-plane for different anomalous viscosity factors. The anomalous viscosity is in units of $R_o^2 B_o^2 h$. (b) Vertical magnetic fields at the mid-plane for different anomalous viscosity factors are compared to those measured by the internal probe.

Current address : General Atomics, San Diego, CA

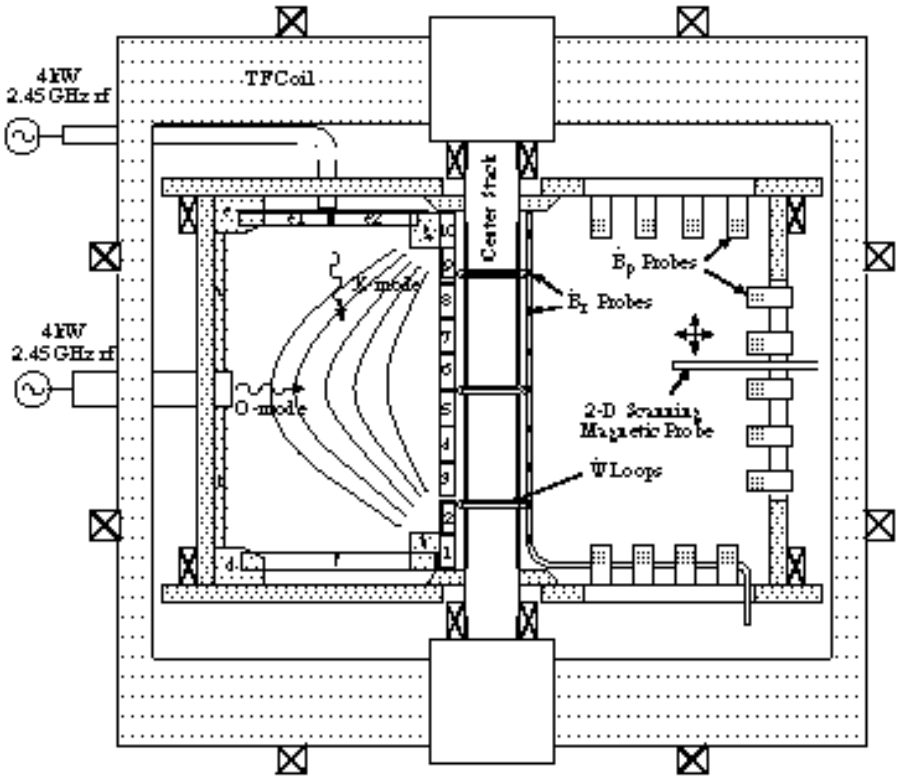
4kW
2.45 GHz rf
TF Coil
Center Stack
X-mode
4kW
2.45 GHz rf
O-mode
$\dot{B}_p$ Probes
$\dot{B}_r$ Probes
2-D Scanning
Magnetic Probe
$\dot{W}$ Loops

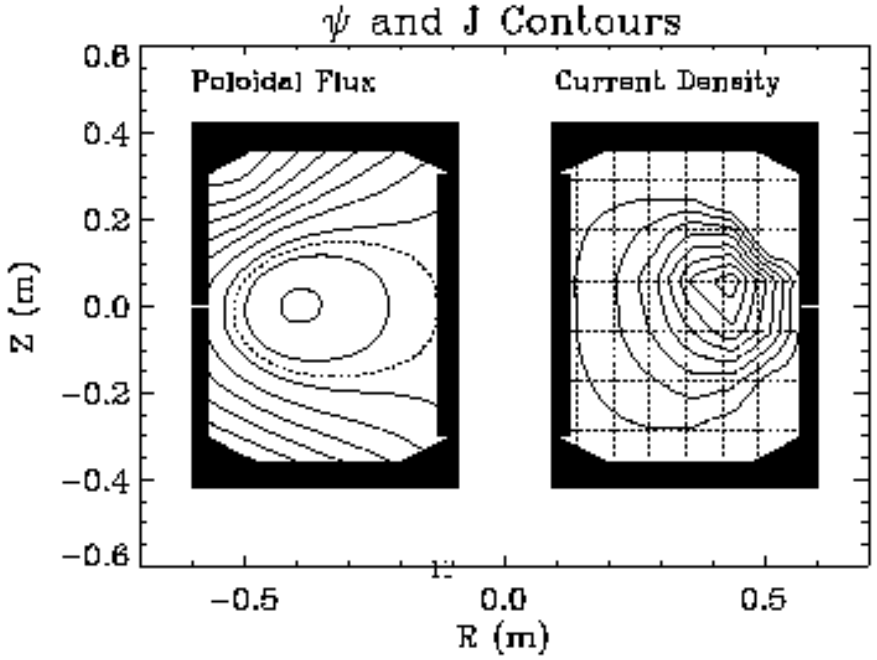
ψ and J Contours
Poloidal Flux
Current Density
Z (m)
R (m)
0.6
0.4
0.2
0.0
−0.2
−0.4
−0.6
−0.5
0.0
0.5

Figure 1:

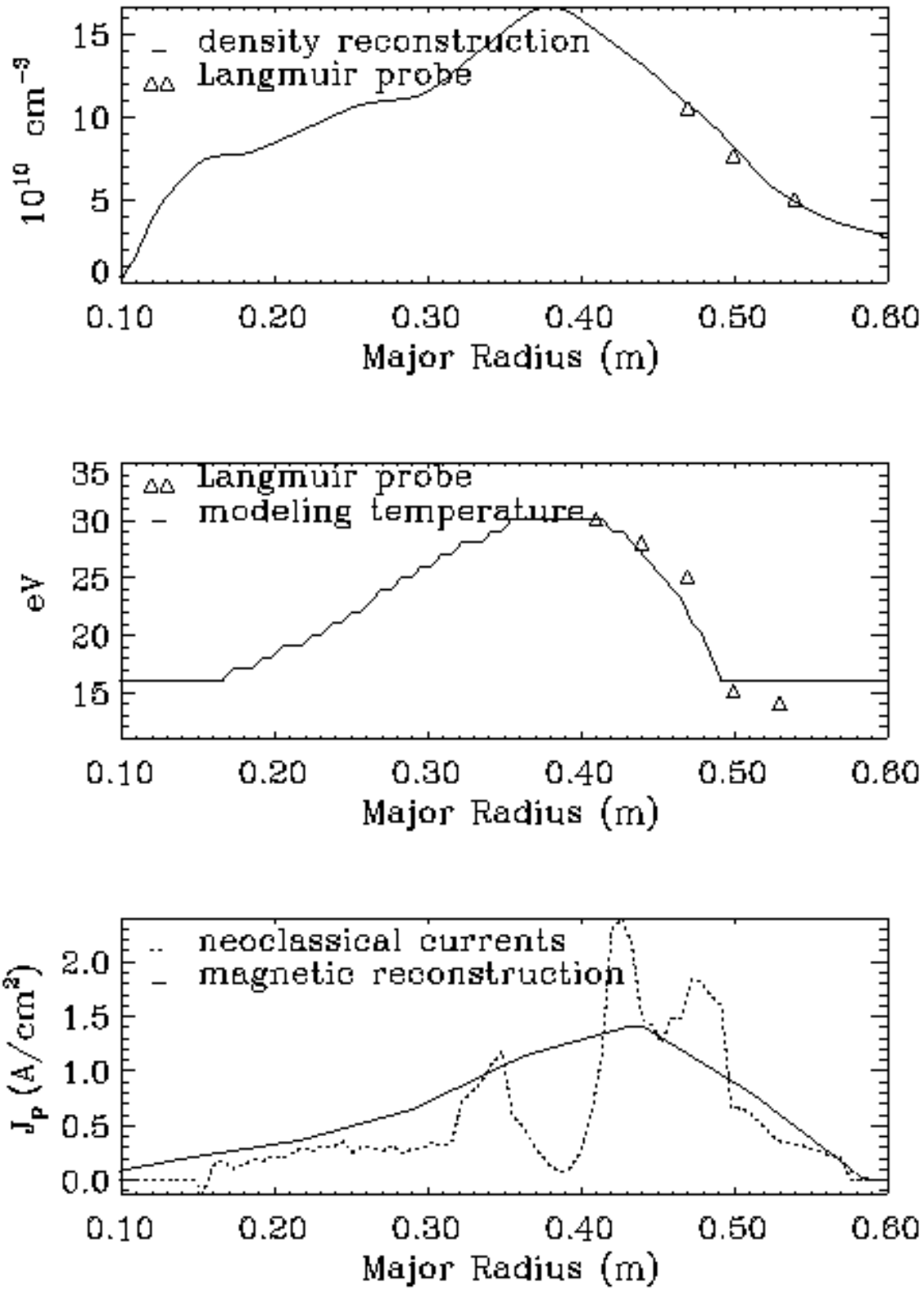
density reconstruction
Langmuir probe
10^{19} cm^{-3}
Major Radius (m)
Langmuir probe
modeling temperature
eV
Major Radius (m)
neoclassical currents
magnetic reconstruction
J_p (A/cm^2)
Major Radius (m)

Figure 2

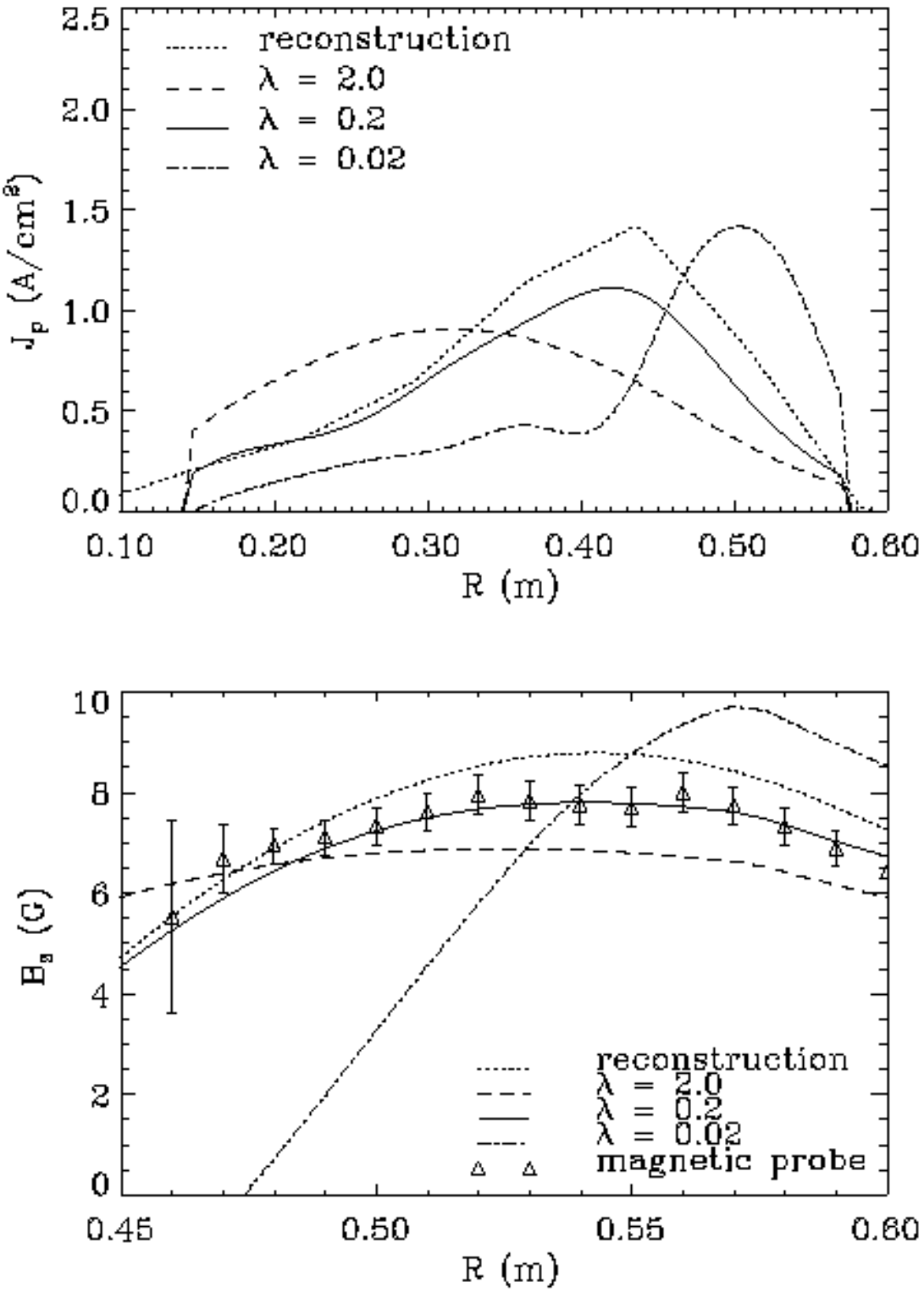

Figure 3